RiESTech
Recent in Engineering Science and Technology

MBI

Article

The Remanufacturing of Track Rollers Requires The Application of A Hardfacing Technique, Which is Achieved by Combining Buttering with 309LMo Gas Metal Arc Welding (GMAW) and The TiC-O Flux-core Arc Welding (FCAW) Process.

Addin Aristotika [1,*], Winarto Winarto [1,*], Sabandi Ismadi [1], Eddy S. Siradj [1], Muhammad Anis [1]

[1] Department of Metallurgical and Materials Engineering, Universitas Indonesia, Depok 16424, Indonesia
* Correspondence: add.in412@gmail.com; winarto.msc@ui.ac.id

Abstract: The operation of the track rollers is dependent on the frictional forces between the rollers and the track. Furthermore, the presence of moisture-laden sand and mud in the surrounding environment accelerates the corrosion process, leading to a synergistic effect on abrasion wear. The production of new rollers is a highly energy-intensive process, resulting in the emission of significant quantities of carbon dioxide. The main objective of this research was to develop a process for remanufacturing track rollers by integrating hardfacing methods, specifically, combining buttering with gas-metal-arc welding (GMAW) that utilizes 309LMo and flux-core arc welding (FCAW) employing TiC-O. During the GMAW process, currents of 180 A, 220 A, and 260 A were applied at the same time as wire with a diameter of 1.2 mm, whereas the FCAW process involved using currents of 200 A, 250 A, and 300 A in conjunction with a wire with a diameter of 1.6 mm. An evaluation was conducted through mechanical tests and metallurgical analysis to determine the effect of the variable current on the physical and mechanical properties of the hardfill layer. Mechanical tests using the Rockwell method and metallurgical analysis via morphological observation were conducted to assess the performance of the remanufactured track roller. The outcomes revealed that as the current increase in GMAW/FCAW welding, the hardfacing layer became increasingly stiffer, but this effect was offset by the failure of the hardfacing interface to bond correctly, as shown by its insufficient fusion and the formation of cracks and holes that penetrated into the base metal. This study highlights the importance of welding parameters to achieve a balance between hardness in the base and weld metals, diffusion, and the quality of the bond between the two, as a practical and cost-efficient method for the remanufacturing industry.

Keywords: Remanufacturing; Track Rollers; Hardfacing; Buttering; 309LMo; GMAW; FCAW

Citation: Aristotika, A., Winarto, Ismadi, S., Siradj, E. S., Anis, M. (2025). The Remanufacturing of Track Rollers Requires The Application of A Hardfacing Technique, Which is Achieved by Combining Buttering with 309LMo Gas Metal Arc Welding (GMAW) and The TiC-O Flux-core Arc Welding (FCAW) Process. Recent in Engineering Science and Technology 3(03), 40–53. Retrieved from https://www.mbi-journals.com/index.php/riestech/article/view/117

Academic Editor: Noor Hidayati

Received: 10 June 2025
Accepted: 5 July 2025
Published: 31 July 2025

Publisher's Note: MBI stays neutral with regard to jurisdictional claims in published maps and institutional affiliations.

1. Introduction

The track rollers function by applying frictional forces between the roller and the track, thereby inducing wear and thinning of the component. In areas where bulldozers operate in the middle of wet sand and mud, the rollers are susceptible to corrosion. This, in turn, will result in a synergistic effect on abrasion wear. It has been demonstrated that this corrosion cannot be mitigated through the process of hardening the steel. Other surface treatments on the roller, such as carburizing and nitriding, or more conventional methods, are

not cost-effective and insufficient for highly wear-prone and corrosive environments encountered during roller use [1]. Substituting expensive materials like high-alloy steels or other cutting-edge materials is impractical because it significantly increases costs without a matching improvement in performance. Consequently, these materials cannot be considered efficient solutions. The disposal of worn rollers and subsequent manufacturing of new rollers require substantial investment in time and financial resources. The production of new rollers is a highly energy-intensive process, resulting in significant carbon dioxide emissions. As a result, the industry has widely adopted overlay welding or hardfacing techniques to extend the service life of worn components and reduce the wear of machine parts [2]. Plasma transfer arc welding, gas metal arc welding, gas tungsten arc welding, shielded metal arc welding, flux-core arc welding, and submerged arc welding are employed for hardfacing [3].

The primary goal of hardfacing is to reduce wear by applying a hard, abrasion-resistant coating to a component's surface via welding or a comparable process. Hard metal compounds, which combine carbide and metal, are used to increase the lifespan of machine components [4]. The accumulation of wear-resistant deposits on the metal surface increases the service life of the material. The hardfacing process involves the incorporation of metal–alloy powders into the material surface. The hardfaced metal parts become hard and exhibit increased wear resistance. The use of wear-resistant coatings requires the process of carburization to be carried out. On the other hand, previous studies have found that the oxidation of wear-resistant coatings during subsequent carburizing processes can have a negative impact on their ability to withstand wear [1]. Although the primary function of hardfacing is to restore worn components to a state of functionality, hardfacing is also employed in new-component pre-use applications. Hardfacing materials can extend their lifespan, providing additional benefits, such as increased operational efficiency, decreased need for replacement parts, and the use of less expensive base metals, ultimately resulting in moderate costs [3].

The welding process employed in this study was the FCAW method. Flux-core arc welding, or FCAW, is highly versatile and widely used due to its user-friendly nature, high current density, and ability to deposit significant amounts of weld metal by using multiple wires simultaneously. This is a significant benefit in the manufacturing sector, particularly because of the capacity to restore worn components [5]. FCAW has been identified as a particularly suitable process for overlay manufacturing because of its high productivity and deposition rate [2]. FCAW has been shown to be a superior method to other techniques due to its notable advantages, which include ease of controlling process variables, high-quality results, achieving deep penetration, yielding a smooth finish, accommodating thicker parts, and preventing contamination from the environment [6]. A significant advantage of the FCAW process is that once the initial operational phase has been completed, the operator skills required are substantially less complex than those required for manual processes. The employment of advanced technology in FCAW is the reason for the process's capacity for automatic operation, thereby enhancing its productivity.

The FCAW process has been found to produce carbides that significantly enhance the base metal's properties, such as mechanical strength, where a harder weld metal correlates with increased wear resistance, as well as corrosion and creep resistance [7].

The track roller that is the subject of this study is composed of a material known as SMnCrMoB435H. This material is classified as a medium-carbon steel, and it finds application as a tool steel. This material is produced through a continuous cooling process known as sinter hardening, which results in the formation of a bainitic microstructure within the steel. The presence of manganese and chromium (both of which have a high affinity for oxygen) and Mo will increase the hardenability of the steel. These elements have been shown to promote the formation of hard phases such as bainite and martensite [8]. The formation of both phases is also facilitated by the formation of borides. Furthermore, borides exhibit high hardness properties and good wear resistance [9]. Nickel is often replaced by manganese, which has proven to be up to four times more effective than nickel and also significantly more affordable, as noted by Sulowski in 2008 [10], thereby enhancing hardness.

This research aims to clarify the effects of hardfacing on PT X track roller components, specifically those arc-welded with flux-core technology, in terms of hardness distribution and their influence on previous problems in an effort to establish the key parameters required for achieving high-quality welding outcomes.

2. Materials and Experiment Methods

The specimen employed in this study was SMnCrMoB435H steel with dimensions of 220 millimeters in diameter and 50 millimeters in thickness. The welding process employed 309LMo stainless steel electrodes with a diameter of 1.2 mm for gas metal arc welding (GMAW) and the hardfaced TIC-O electrodes with a diameter of 1.6 mm for flux-core arc welding (FCAW). The samples were cleaned using a wire brush. The SMnCrMoB435H steel plate was welded using a combination of the GMAW and FCAW methods at constant voltage and speed. The variable currents used in both welding processes were 180/200 A, 220/250 A, and 260/300 A. These currents are referred to as samples A, B, and C, respectively.

Following the welding process, the samples were subjected to observation and evaluation procedures. Visual observation is required to ensure that the thickness of the hardfacing layer meets the minimum requirements for the track-rollers component. A scanning electron microscope (SEM) was used to perform sample observations to determine its microstructure. Energy-dispersive x-ray spectroscopy (EDS) was used for layer composition testing. Hardness testing is a type of mechanical test performed using the Vickers method with a load of 150 kg and a dwell time of 15 seconds.

3. Results and Discussion

3.1. Visual Observation

The thickness of the welding output was measured during the observation. Measurements were performed by determining the minimum and maximum thickness of each sample. The weld thickness was measured using a thickness gauge.

The findings of a welding thickness measurement study are detailed in Table 1 which contains the lists of the weld thicknesses at each variation in the welding current. The largest weld thickness (3.5 cm) was obtained for sample A. The maximum thickness of samples B and C was 3 cm. The maximum thickness of the three samples remained relatively consistent, primarily due to the welding current staying within the specified range outlined in the technical documentation for the welding wire. The minimum thickness of the hardfacing layer, as per the manufacturing requirements, must be 1.1 cm. According to visual observation, the resulting thickness fell within the range of 2.5 to 3.0 cm. The thickness complies with the manufacturing requirements. The excess thickness is intended to facilitate further manufacturing processes such as machining.

Table 1. The thickness measurement of the welding outcome.

Sample Code	Thickness (cm)	
	Min.	Max.
A	2.5	3.5
B	2.5	3
C	2.5	3

3.2. Scanning Electron Microscope (SEM) Analysis

A SEM analysis was performed to examine the bond interfaces (fusion lines) both between the hardfacing layer and the base metal and the phases produced during the welding process. As shown in Figure 1, sample A exhibits a clear and continuous transition between the hardfacing layer and the base material. There was no significant porosity or cracking, indicating good metallurgical bonding. The formation of elongated formations that penetrate the base material suggests sufficient diffusion and bonding. The microstructure exhibits good welding parameters with optimized interlocks and minimal mixing effects.

In sample A (Figure 1), the phase likely formed in the hardfacing layer is probably martensite, as evidenced by the needle-like and smooth morphology. This phase is formed by rapid cooling after the welding process. This finding aligns with the results of the EDS test conducted on sample A, which revealed the composition of the Fe-Cr-Ni-Mo hard coating. The possible phases of the base metals include pearlite and ferrite. Additionally, the presence of bainite or partial martensite at the interface is a possibility, owing to the heat effect of welding.

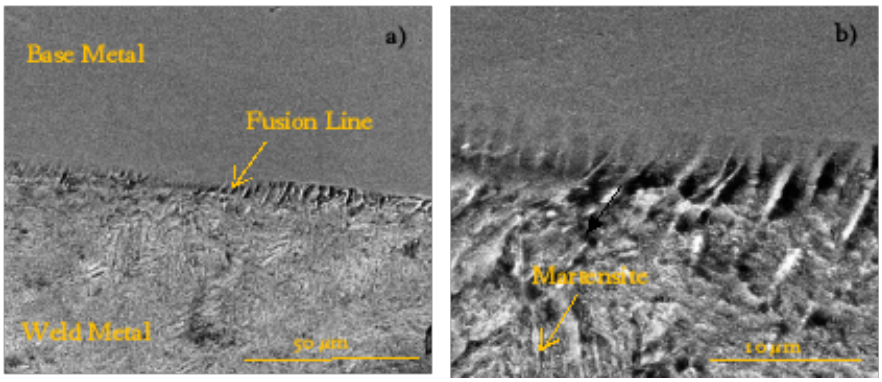

Figure 1. The interface bonding microstructure of sample A (180/200 A)

In sample B, as illustrated in figure 2, the interface layer exhibits substantial defects, including cracks and voids that extend into the base metal. The presence of these defects indicates a weakened interfacial bond (fusion line), which can result in premature failure under mechanical loading. The rough interface layer is a result of high heat input caused by the increased current, leading to excessive dilution of the welding wire, which in turn compromises the overall bond integrity[11].

As illustrated in Figure 2, the phase formed in the hardfacing layer of sample B is martensite, as evidenced by its needle-like and smooth morphology. This phase is quenched by rapid cooling after the welding process. The possible phases of the base metals include pearlite and ferrite. Additionally, the presence of bainite or partial martensite at the interface is a possibility, owing to the heat effect of welding.

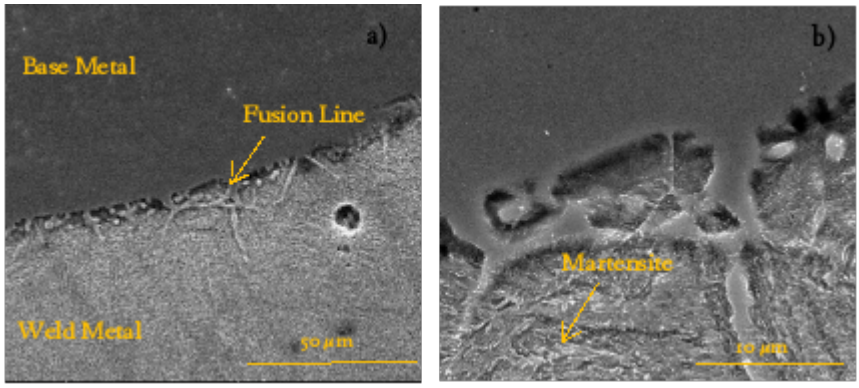

Figure 2. Interface bonding microstructure of sample B (220/250 A)

In sample C (Figure 3, the interfacial layer shows moderate bonding quality, with some areas showing interdiffusion but also visible cracks and porosity. The formation of irregular dendritic structures indicates that high heat input altered the integrity of the microstructure [12]. The presence of micro-cracks can be attributed to two factors: thermal expansion mismatch and the effect of over melting of the welding wire too quickly. Results from the Vickers test show that although the hardness distribution is still relatively high, potential performance degradation and long-term failure can arise from defects in the interface layer. Similar to samples A and B, sample C in Figure 3 also shows the formation of the martensite phase in the hardfacing layer. With regard to the base metal is likely

pearlite, ferrite, and potentially partial martensite. The presence of chromium and molybdenum carbide was detected, and these elements contributed to enhancing both strength and ductility. The presence of chromium, manganese, and iron in the base metal is also supported by the results of the EDS test carried out on sample C.

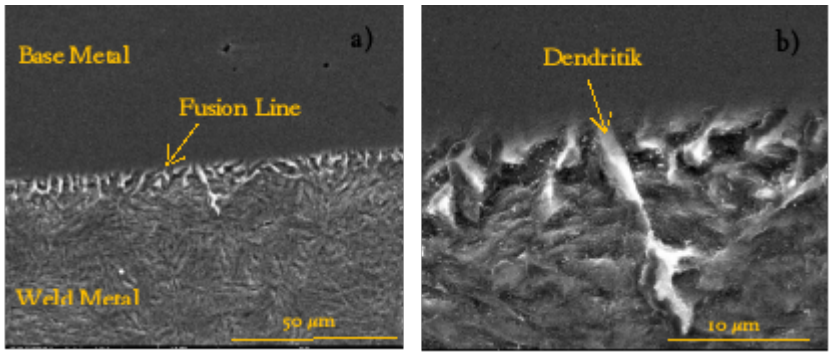

Figure 3. Interface bonding microstructure of sample C (260/300 A)

The microstructural observations were consistent with the hardness values obtained from the Vickers test results (see Table 2). As demonstrated by the microstructure, Sample A exhibited the most uniform and well-bonded interface layer. This particular sample showed a balanced distribution of hardness, with readings spanning from 195 to 233 HV. In contrast, sample B, which displayed visible imperfections, had higher hardness values (216 - 235 HV) but a non-uniform interface bonding layer. As illustrated in Figure 1, sample C, which exhibited the most substantial welding current, exhibited moderate hardness (230 – 223 HV). The microstructural analysis showed discrepancies in the interface layer, which implies a lack of fusion occurred. The presence of cracks in samples B and C indicates that increasing the welding current can cause excessive heat input, thermal stress, and structural defects, reducing the overall strength of the interface [13]. The analysis of sample A reveals a microstructure that strikes a balance between the mechanical properties and the presence of a robust interface layer, indicating optimization. This observation indicates that samples exhibiting such characteristics are probably optimal for the given study parameters.

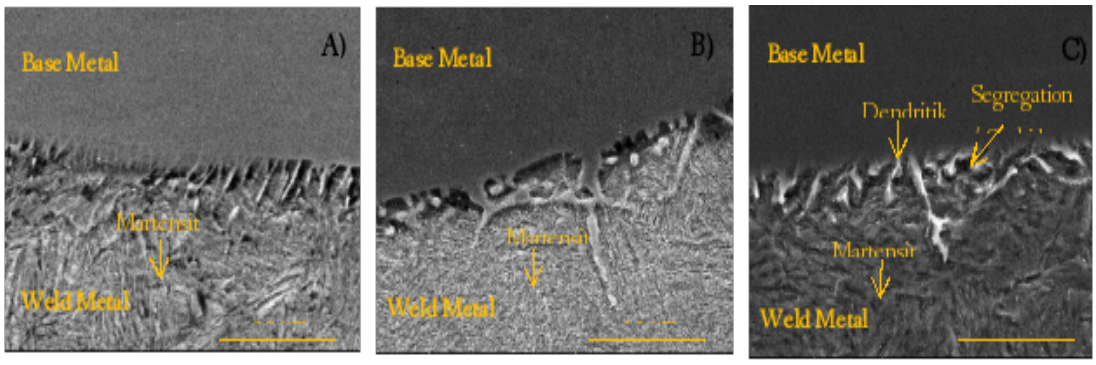

Figure 4. Microstructure comparison of samples A (180/200 A), B (220/250 A), and C (260/300 A)

3.3. Energy-dispersive X-ray Spectroscopy (EDS) Analysis

The EDS data for sample A (Figure 5) shows that the Fe-Cr-Ni-Mo hard coating composition is consistent with the chromoly steel base material and the wear-resistant coating. The presence of chromium and molybdenum has been pinpointed as a key factor in carbide formation, which in turn contributes to increased hardness. In addition, nickel (Ni) plays a crucial role in ensuring toughness [14].

The EDS test results analysis revealed that Sample A's hardfacing layer was made up of either low-alloy steel or mild steel, which was confirmed by the presence of iron (~97%) with small amounts of manganese and chromium. The absence of substantial concentrations of chromium and molybdenum in the hardfacing layer results in its deficient natural hardness and wear resistance.

Figure 7 shows the EDS test results for the base metal part of sample B. The base metal part of sample B had higher concentrations of chromium (18.82 wt.%) and nickel (12.51 wt.%) than sample A (16.49 wt.% Cr and 10.64 wt.% Ni). This led to enhanced wear resistance, toughness, and corrosion resistance. The slight increase in Mn in sample B also contributed to the improvement in the mechanical properties. This improvement is evident in the Vickers hardness test results, where the hardness test results of sample B are higher (216 HV) than those of sample A (195 HV). These results show that sample B may outperform sample A for applications requiring high wear resistance and impact toughness. However, the microstructure analysis results show that the interface layer of sample A is superior to that of sample B (it has no defects and is fused).

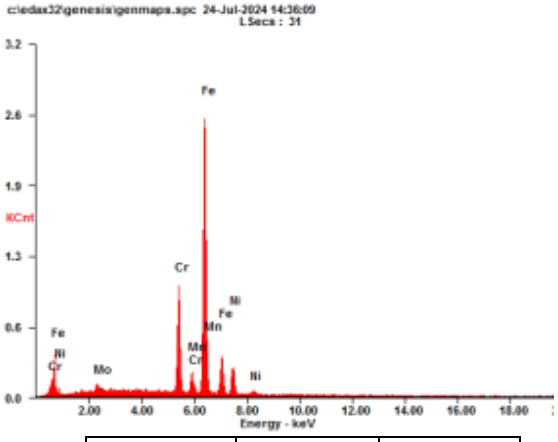

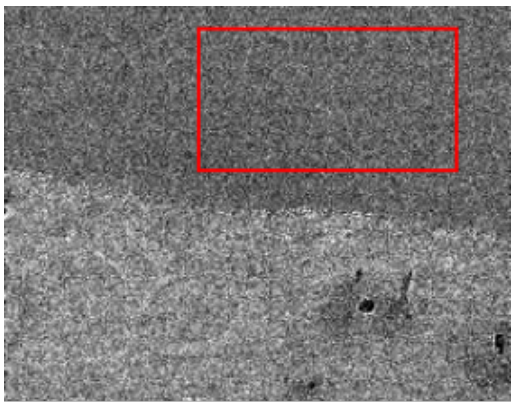

Element	*wt.%*	*at.%*
MoL	02.09	01.22
CrK	16.49	17.74
MnK	01.74	01.77
FeK	69.04	69.14
NiK	10.64	10.13
Matrix	Correction	ZAF

Figure 5. EDS results for base metal sample A (180/200 A)

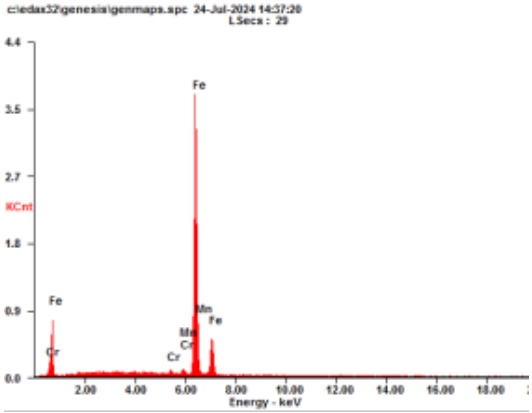

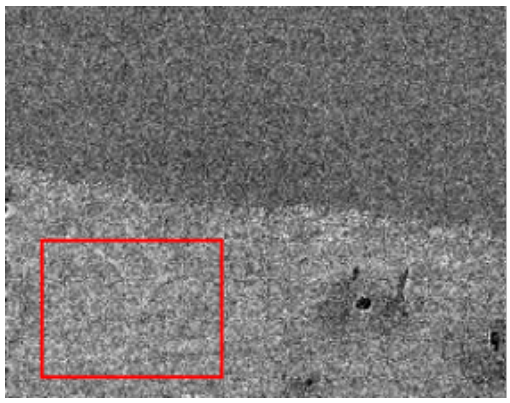

Element	*wt.%*	*at.%*
CrK	01.00	01.08
MnK	01.70	01.72
FeK	97.30	97.20
Matrix	Correc-tion	ZAF

Figure 6. EDS **results** on the hardfacing layer of sample A (180/200 A)

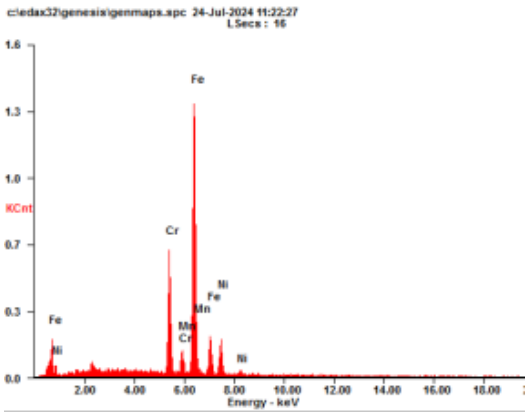

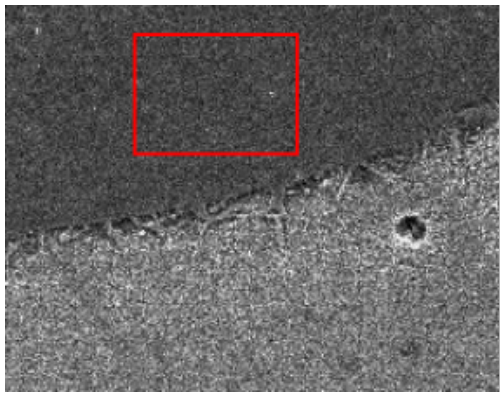

Element	*wt.%*	*at.%*
CrK	18.82	20.05
MnK	02.20	02.21
FeK	66.48	65.94
NiK	12.51	11.80
Matrix	Correc-tion	ZAF

Figure 7. EDS results for base metal sample B (220/250 A)

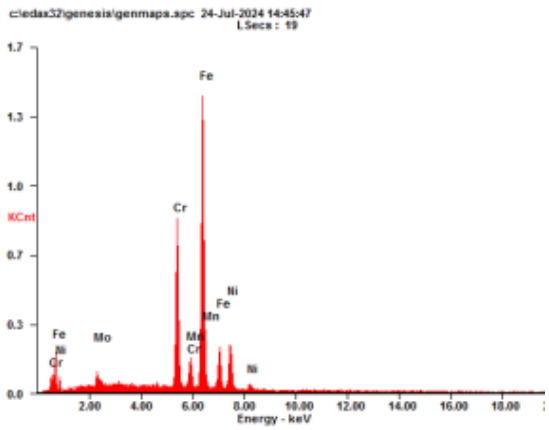

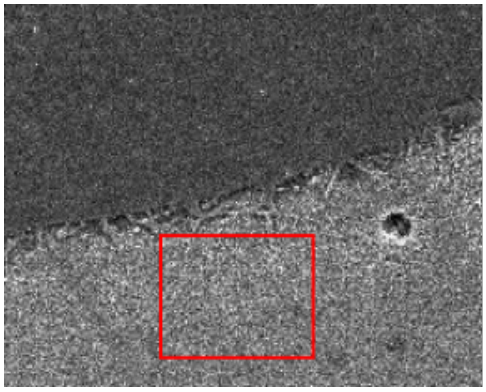

Element	*wt.%*	*at.%*
CrK	01.13	01.21
MnK	01.85	01.88
FeK	97.02	96.91
Matrix	Correc-tion	ZAF

Figure 8. EDS results on hardfacing layer B (220/250 A)

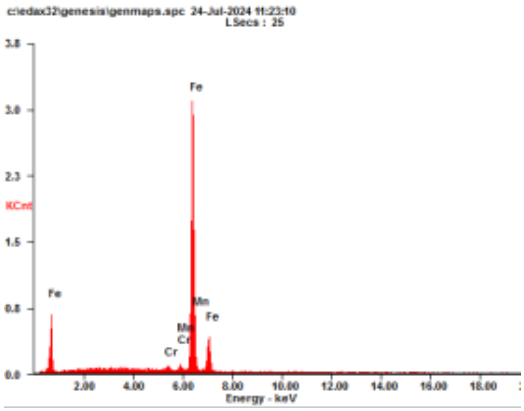

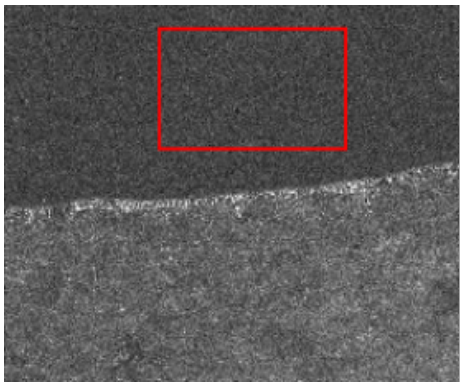

Element	*wt.%*	*at.%*
MoL	03.24	01.89
CrK	22.40	24.15
MnK	01.92	01.96
FeK	57.49	57.72
NiK	14.94	14.27
Matrix	Correc-tion	ZAF

Figure 9. EDS results for base-metal sample C (260/300 A)

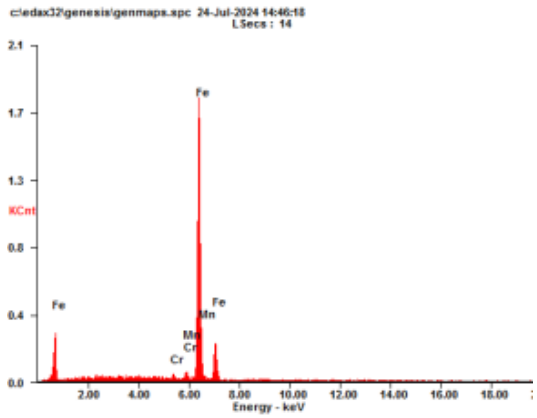

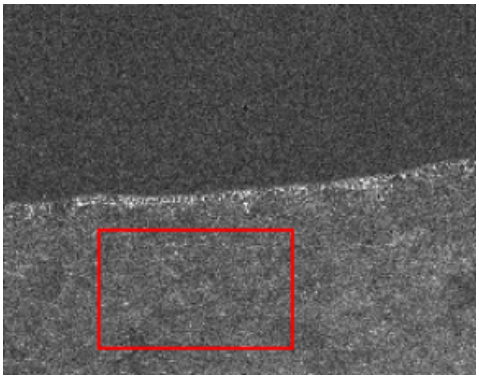

Element	*Wt.%*	*At.%*
CrK	00.97	01.04
MnK	02.21	02.24
FeK	96.82	96.72
Matrix	Correc-tion	ZAF

Figure 10. EDS results on hardfacing layer sample C (260/300 A)

The EDS test results for sample B's hardfacing layer (Figure 8) reveal that this layer is identical to that in sample A, comprising low alloy steel with very small amounts of Cr and Mn, rendering it vulnerable to wear and corrosion [15].

The EDS test results for the base metal of sample C (Figure 9) indicated the presence of Cr, Ni, Mo, Mn, and Fe elements. The test results for the hardfacing layer in sample C, as shown in Figure 10, are comparable to those of samples A and B, both of which had a hardfacing layer consisting mainly of iron-based steel with low chromium (Cr) and moderate manganese (Mn) content. This is consistent with the established specifications for hardfacing welding wire. The base metal part exhibits a substantial enhancement in resistance to wear and corrosion, which is attributable to its elevated concentrations of Cr, Ni, and Mo.

3.4. Hardness Test Analysis

The primary goal of hardness testing is to determine the variations in hardness within the weld area and the surrounding regions, which may be affected by the welding process, including the area influenced by heat and the base metal itself. The outcomes of the hardness test are presented in Table 2. The hardness value was determined in five distinct regions: the hardfacing layer area (areas I and II) and the base metal area (areas III, IV, and V). As shown in Table 2, the hardfacing layer exhibits a lower degree of hardness than the base metal. Conversely, in the domain of welding, it is anticipated that the hardness produced in the hardfacing layer is expected to exceed that of the base metal [16].

Table 2. Hardness test results of the hardfacing layer are expressed in HV.

Sample Code	Welding Current (A)	Hardness Value of the Tracing Area (HV)						
		Hardfacing			Base Metal			
		I	II	Average	III	IV	V	Average
A	180/200	194	196	195	238	233	227	233
B	220/250	216	216	216	237	239	230	235
C	260/300	229	232	230	225	222	222	223

In addition to examining the hardness distribution, hardness testing was conducted to determine the effect of increasing the current during the welding process. The hardness values (HV) of hardfacing and base metal are shown in Figure 11, with three unique welding current variations: 180/200 A for sample A, 220/250 A for sample B, and 260/300 A for sample C.

As demonstrated in Tabel 2, sample A exhibited the lowest surface-layer hardness (195 HV). Research has indicated that at lower currents, the layer formed may not undergo sufficient heat or significant dissolution, resulting in a relatively less rigid structure [15]. Sample B exhibited a high-hardness layer (216 HV), this observation signifies that the application of the welding current is adequate for promoting superior heat, resulting in a more refined microstructure. This, in turn, led to the enhancement of wear resistance. As indicated by the higher hardness value (230 HV) of sample C produced an increased hardness layer compared to sample B. The welding process-generated heat energy is also a contributing factor to the enhanced material melting and the strengthened bond between particles within the hardfacing layer. Increased heat input results in the formation of refined microstructure grains. The refined microstructure contains more grain boundaries, which hinder the movement of dislocations, ultimately resulting in increased material hardness [15].

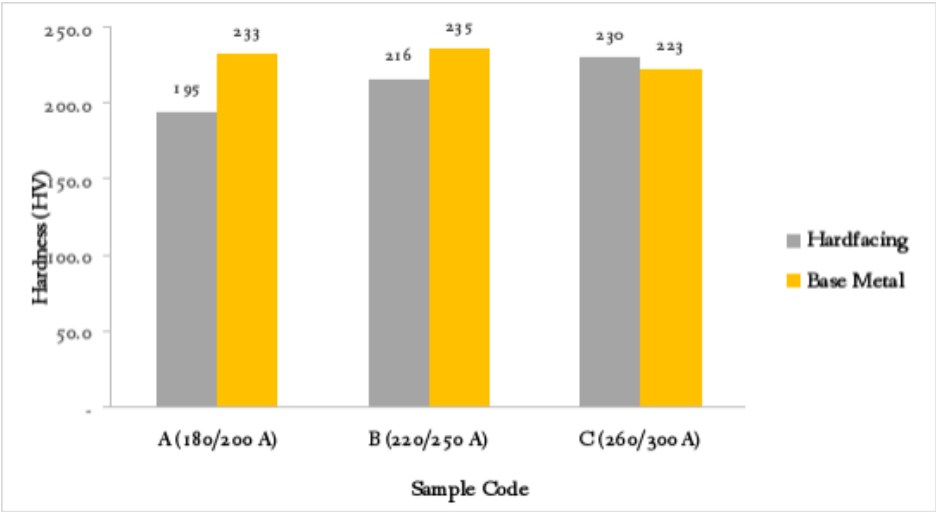

Figure 11. Effect of welding parameters on coating hardness

In the case of base metals, the effect of increasing the current on the hardness is not significant. The Vickers test results demonstrated that Sample A (233 HV) yielded the highest base metal hardness, indicating the least softening of the heat-affected zone (HAZ). An increase in the welding current resulted in a slight rise in the base metal hardness of Sample B, as indicated by an increase of 235 HV. This phenomenon can be attributed to the broader heat input exerting its influence on the HAZ. The increased heat resulted in a greater degree of austenitization of the base metal. During the rapid cooling process, when the cooling rate remains high, martensite formation is enhanced. In sample C, an increase in the welding current decreased the base metal hardness (230 HV). This indicates that an increase in the heat input can reduce the cooling efficiency, particularly in cases where the thermal mass is substantial. Slow cooling will form ferrite and pearlite phases, reducing the hardness.

Higher welding currents generally increases hardfacing hardness up to a point. Research findings suggest that the hardness of samples A, B, and C are associated with higher thermal energy levels, which are produced by higher currents, resulting in a faster fusion process and a stronger metallic bond between layers [17]. Following the welding process, the surface layer cools rapidly, resulting in the formation of denser microstructures, specifically martensite and hard phases featuring carbides or intermetallic, which emerge as a consequence of the high thermal condition during welding. The metal's hardness diminished slightly as the welding current increased, mainly due to thermal effects, which probably softened the microstructure within the heat-affected zone. The hardness of sample C (220/250 A) showed the best balance, achieving hardness (230 HV) while maintaining balance with the base metal (223 HV). Unfortunately, sample C did not exhibit a good interface layer, as observed under a microscope. Among the examined samples, sample C had an appropriate hardness value for the hardfacing layer, meeting the expected manufacturing requirements of at least 230 HV.

4. Conclusions

The process of hardfacing the SMnCrMoB435H material using mixed-metal arc welding (GMAW)/flux-core arc welding (FCAW) to the hardness profile was examined. It was observed that as the current increased in the MIG/FCAW welding, the hardfacing layer became harder. However, this is not supported by the interface bond, which does not appear to be fused. Cracks and holes that propagate to the base metal are also present.

FCAW welding of the track roller dimensions has a substantial impact on the microstructure of SMnCrMoB435H steel, which is subjected to GMAW-FCAW welding. The thickness of the hardfacing layer was found to be a minimum of 2.5 centimeters, which exceeds the targeted thickness of 1.1 centimeters.

In this study, the influence of welding current on the interfacial quality and mechanical performance of hardfacing layers was investigated. Sample A (180/200 A) exhibited optimal interface quality, as indicated by the uniform interface bonding and the absence

of significant defects. Conversely, Samples B and C exhibited signs of cracking and porosity, indicating that elevated current levels resulted in excessive heat input, leading to undesirable structural degradation. Furthermore, the hardness of the hardfacing layer reached 230 HV in sample C, which is in accordance with the targeted hardness specification. It is imperative to optimize welding parameters to achieve a balance between hardness, diffusion, and interface bonding quality to enhance durability in industrial applications.

Author Contributions: "Conceptualization, W.W.; methodology, W.W., A.A., S.I.; formal analysis, W., A.A., S.I; writing—original draft preparation, A.A.; writing—review and editing, W.A., E.S., M.A.; visualization, A.A.; supervision, W.W., E.S., M.A.; All authors have read and agreed to the published version of the manuscript."

Funding: This study received no specific funding from government, commercial, or non-profit organizations.

Acknowledgments: The authors would like to acknowledge the testing laboratory of the Center for Materials Processing and Failure Analysis, Universitas Indonesia, Depok, Indonesia, for its support and facilities. Appreciation is also extended to the Laboratory in Area Science and Technology B.J. Habibie, National Research and Innovation Agency (BRIN), Serpong, for valuable assistance and access to its research infrastructure.

Conflicts of Interest: The authors declare no conflict of interest.

References

1. T. D. Wodrich, Reinhard Jordan, and Alois Kroll, "Track chain link and undercarriage track roller having a metallurgically bonded coating," US 7,657,990 B2, 2006 Accessed: Dec. 11, 2024. [Online]. Available: https://patentimages.storage.googleapis.com/9d/11/c0/e2c6191f4b9e01/US7657990.pdf
2. P. F. Mendez *et al.*, "Welding processes for wear resistant overlays," *J Manuf Process*, vol. 16, no. 1, pp. 4–25, 2014, doi: https://doi.org/10.1016/j.jmapro.2013.06.011.
3. D. Tandon, H. Li, Z. Pan, D. Yu, and W. Pang, "A Review on Hardfacing, Process Variables, Challenges, and Future Works," *Metals (Basel)*, vol. 13, no. 9, 2023, doi: 10.3390/met13091512.
4. S. N. I. M. V. G. I. F. and D. L. O. Neikov, *Handbook of Non-Ferrous Metal Powders*. Elsevier, 2019. doi: 10.1016/C2014-0-03938-X.
5. A. Patnaik, S. Biswas, and S. S. Mahapatra, "An evolutionary approach to parameter optimisation of submerged arc welding in the hardfacing process," *International Journal of Manufacturing Research*, vol. 2, no. 4, p. 462, 2007, doi: 10.1504/IJMR.2007.015089.
6. A. Rehal and J. S. Randhawa, "Submerged Arc Welding Fluxes-A Review," *International Journal of Science and Research*, 2014, doi: 10.21275/02014158.
7. B. Gülenç and N. Kahraman, "Wear behaviour of bulldozer rollers welded using a submerged arc welding process," *Mater Des*, vol. 24, no. 7, pp. 537–542, Oct. 2003, doi: 10.1016/S0261-3069(03)00082-7.
8. M. Sulowski and A. Cias, "Microstructure and properties of Cr-Mn structural steels sintered in a microatmosphere," *Proceedings of the World Powder Metallurgy Congress and Exhibition, World PM 2010*, vol.

3, Dec. 2010.

9. L. L. Silveira, A. G. M. Pukasiewicz, G. B. de Souza, P. Soares, and R. D. Torres, "Effects of boron concentration on the microstructure, mechanical and tribological properties of powder-pack borided AISI 4140 steel," 2022. [Online]. Available: https://api.semanticscholar.org/CorpusID:246570209
10. M. Sulowski, "DILATOMETRIC INVESTIGATION OF Fe-Mn-Cr-Mo PM STEELS WITH DIFFERENT CARBON CONCENTRATIONS," 2008.
11. B. Derbiszewski, A. Obraniak, A. Rylski, K. Siczek, and M. Wozniak, "Studies on the Quality of Joints and Phenomena Therein for Welded Automotive Components Made of Aluminum Alloy—A Review," May 01, 2024, *Multidisciplinary Digital Publishing Institute (MDPI)*. doi: 10.3390/coatings14050601.
12. Niraj Kumar, Chandan Pandey, and Prakash Kumar, "Dissimilar Welding of Inconel Alloys With Austenitic Stainless-Steel: A Review," *J. Pressure Vessel Technol.*, vol. 145, no. 1, p. 011506, Feb. 2023.
13. Y. Q. Liu, D. Yu, Y. Zhang, J. P. Zhou, D. Q. Sun, and H. M. Li, "Research advances on weldability of Mg alloy and other metals worldwide in recent 20 years," Jul. 01, 2023, *Elsevier Editora Ltda*. doi: 10.1016/j.jmrt.2023.06.184.
14. H. Oktadinata, W. Winarto, D. Priadi, E. S. Siradj, and A. S. Baskoro, "Impact toughness characteristics of sm570-tmc steel joint using welding wire containing 0.4% nickel at different level of heat input," in *Key Engineering Materials*, Trans Tech Publications Ltd, 2020, pp. 117–124. doi: 10.4028/www.scientific.net/KEM.867.117.
15. S. Kou, "WELDING METALLURGY SECOND EDITION," 2003. [Online]. Available: www.copyright.com.
16. W. Winarto, M. Anis, and T. P. Hertanto, "Mechanical Properties and Microstructure of Welded Dissimilar Metals Using Buttering & Non-Buttering Layer," *Adv Mat Res*, vol. 0, pp. 341–346, Sep. 2013, doi: 10.4028/www.scientific.net/amr.0.341.
17. by Winarto and D. Priadi, "Effect of Preheating and Buttering on Cracking Susceptibility and Wear Resistance of Hardfaced HSLA Steel Deposit *," *Yosetsu Gakkai Ronbunshu/Quarterly Journal of the Japan Welding Society*, vol. 31, no. 4, pp. 202–205, 2013.